

## Far-infrared optical and dielectric response of ZnS measured by terahertz time-domain spectroscopy

L. Thamizhmani, A. K. Azad, Jianming Dai, and W. Zhang<sup>a)</sup>

*School of Electrical and Computer Engineering, Oklahoma State University, Stillwater, Oklahoma 74078*

(Received 6 December 2004; accepted 16 February 2005; published online 23 March 2005)

The optoelectronic technique of terahertz time-domain spectroscopy (THz-TDS) has been applied to measure the frequency-dependent optical and dielectric properties of ZnS in the frequency range extending from 0.3 to 3.5 THz. THz-TDS clearly reveals the low-frequency phonon resonance features in both the single- and polycrystalline ZnS. These phonons account for the increased absorption as indicated by the resonance lines in the spectra. The measured index of refraction is found to be dominated by the transverse optical-phonon resonance, which is verified by a theoretical fit using the relation for the dielectric response of the damped harmonic oscillator. © 2005 American Institute of Physics. [DOI: 10.1063/1.1896451]

As one of the II–VI compounds ZnS is an excellent optical material in the infrared and far-infrared region.<sup>1</sup> It plays a vital role in being used as infrared windows and lenses as tough front optics in thermal imaging systems, especially those exposed to harsh surroundings. ZnS has special applications in missile domes, and space borne systems. With a band-gap energy of 3.6 eV, ZnS is also widely used as the base materials for cathode-ray tube luminescent materials, catalysts, electroluminescent devices,<sup>2</sup> and UV semiconductor lasers for optical lithography. Nanostructures made of ZnS are attractive in applications of electronic and optoelectronic nanodevices<sup>3</sup> and have potential applications in terahertz optoelectronics. It is crucial to precisely characterize the frequency-dependent optical properties and complex dielectric response of ZnS over a broad far-infrared spectral range.

In this letter, we present the measurements of the optical and dielectric properties of single- and polycrystalline ZnS over the frequency range from 0.3 to 3.5 THz using terahertz time domain spectroscopy (THz-TDS). Owing to the high signal-to-noise ratio (S/N), coherent phase detection, and nonionizing properties THz-TDS has shown significant advantages over many of the far-infrared spectroscopy modalities. It has been widely used in characterizing a variety of materials including molecular vapors, semiconductors, superconductors, biomedical molecules and tissues, nanostructures, and artificial metallic structures. Here, the THz-TDS measurements show that the absorption in the ZnS samples is characterized by the low-frequency phonon resonance lines, among which a difference phonon resonance band located at 0.78 THz is observed. These phonon resonances agree well with previous predictions and measurements. The behavior of the index of refraction is determined by the transverse optical (TO) phonon line centered at 8.13 THz and is well fit by the relation for the dielectric response of the damped harmonic oscillator.<sup>4,5</sup> The measured power absorption and refractive index are compared with channel spectrum data,<sup>1</sup> demonstrating that THz-TDS has the ability to determine the optical and dielectric parameters more precisely than the previous work.

The single crystal ZnS sample is an undoped, 10 mm × 10 mm × 1 mm thick, <100> freestanding crystal optically polished on both sides (RMT Ltd., Russia). It was grown from a source of polycrystalline ZnS at temperature of 1100–1250 °C and a pressure of 1 atm in a hydrogen-filled ampoule using the seeded vapor-phase free growth technology.<sup>6</sup> Growth was along the <111> direction and the crystal consists of 96%–98% zincblende structure and only 2%–4% wurtzite structure. The resistivity of the crystal is in the range of 10<sup>8</sup>–10<sup>12</sup> Ω cm. The polycrystalline ZnS sample (Crystan Ltd., UK) is a 25.4 mm × 25.4 mm × 3.42 mm thick, double-side polished slab. It was synthesized from zinc vapor and gaseous hydrogen sulphide, and formed as sheets on graphite susceptors.

The terahertz system used in the measurements is a photoconductive switch based THz-TDS spectrometer<sup>7</sup> consisting of a confocal system with four parabolic mirrors. The 8–F confocal geometry not only ensures excellent beam coupling between the transmitter and receiver but also compresses the terahertz beam to a frequency independent diameter of 3.5 mm. The sample is attached to an aluminum holder and centered over a 4.5-mm-diameter hole in the plate, which defines the optical aperture. Another identical clear hole is used to take reference signal designated as the input pulse.

The frequency-dependent coefficient of power absorption for the ZnS samples is extracted from the experimental data using the well-known amplitude transmission function of a parallel dielectric slab.<sup>8</sup> Because of the relatively clean separation in time between the main transmitted pulse and the first internal reflection, the data analysis was performed on the main pulse only. For this simple case the denominator in the complex amplitude transmission function for the parallel dielectric slab reduces to unity and the frequency spectrum of only the first transmitted pulse shows no oscillation.<sup>8</sup> This approximation enables the determination of the power absorption  $\alpha$  and index of refraction  $n$  of the sample quite accurately.<sup>7</sup>

The experimentally extracted power absorption of single crystal ZnS is plotted in Fig. 1(a). Three prominent resonance lines are observed at 0.78, 2.20, and 2.80 THz, respectively, and are well assigned based on the previous predictions or observations.<sup>1,9–13</sup> The first resonance peak centered

<sup>a)</sup>Electronic mail: wwzhang@okstate.edu

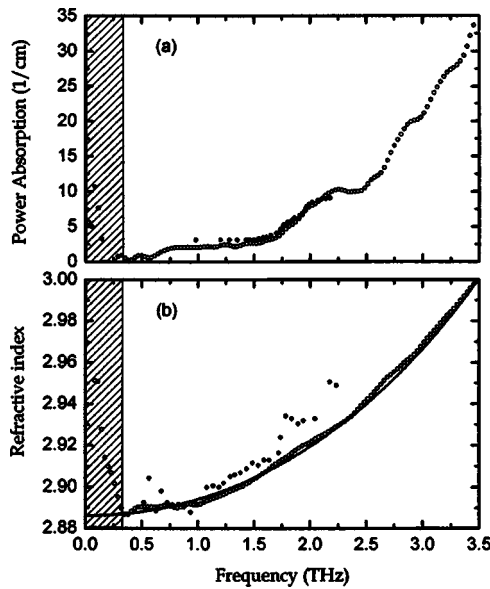


FIG. 1. (a) Comparison of measured results (open circles) for the absorption of single crystal ZnS with the data from Ref. 1 (dots); (b) comparison of measured (open circles) refractive index of single crystal ZnS with the values calculated using the damped harmonic oscillator model (solid line) and the data from Ref. 1 (dots).

at 0.78 THz has lifted the absorption coefficient to  $2 \text{ cm}^{-1}$ . In the Raman measurements this peak was interpreted as a superposition of two difference phonon bands, LA-TA and LO-TO.<sup>9</sup> These phonons were calculated at 88, 110, 306, and  $333 \text{ cm}^{-1}$  for the TA, LA, TO, and LO modes, respectively. The second and broad resonance line with peak power absorption coefficient of  $11 \text{ cm}^{-1}$  is located at 2.20 THz. It is referred to as the transverse TA (L) phonon connecting to two-phonon generation processes of acoustic phonons<sup>10</sup> and was verified with neutron scattering measurements.<sup>11</sup> The resonance feature at 2.80 THz showing peak absorption of  $20 \text{ cm}^{-1}$  was previously observed to be one of the critical-point mode frequencies by neutron scattering measurements at room temperature.<sup>13</sup> It was defined as the TA (X) phonon and was considered as one of the four characteristic zone-boundary phonons used to describe the three-phonon processes in cubic ZnS.<sup>12</sup> In comparison with previous measurements the dots show the room temperature absorption data in the frequency range of 1.0–2.2 THz by channel spectrum technique.<sup>1</sup>

Figure 1(b) shows the frequency-dependent refractive index of single crystal ZnS. Clearly, the measured result represented by open circles also reveals the effect of the phonon resonances that are shown in the power absorption. Similar to ZnTe, the refractive index increases with increasing frequency.<sup>4</sup> This feature is dominated by a high-frequency TO-phonon resonance as predicted in early work.<sup>1</sup> However, compared to the experimental data of ZnTe, the increase in the refractive index of ZnS is not very sharp since the TO-phonon line is centered at 8.13 THz, much higher than 5.32 THz, at which the TO phonon is located for ZnTe. The measured refractive index is theoretically fit using the dielectric response of a damped harmonic oscillator.<sup>4,5</sup> The frequency-dependent dielectric constant in the infrared region for the harmonic oscillator is formulated as  $\epsilon(\omega) = \epsilon_\infty + \epsilon_{st} \omega_{\text{TO}}^2 / (\omega_{\text{TO}}^2 - \omega^2 + 2i\gamma\omega)$ , where  $\omega_{\text{TO}}$  is the transverse optical (TO) phonon frequency,  $\epsilon_\infty$  is the optical dielectric constant,  $\epsilon_{st}$  describes the strength of the TO-phonon resonance at  $\omega_{\text{TO}}/2\pi$ ,  $\epsilon_\infty + \epsilon_{st} = \epsilon_0$  is the static dielectric constant and  $\gamma$  is the damping coefficient. The frequency dependent complex dielectric constant is also given by the square of the complex refractive index,  $n^2 = (n_r + in_i)^2 = \epsilon(\omega)$ . The imaginary part of the index,  $n_i$  can be obtained from  $n_i = \alpha\lambda_0/4\pi$  where  $\alpha$  is the power absorption coefficient, and  $\lambda_0$  is the free-space wavelength. The solid line in Fig. 1(b) shows the theoretical fitting of the measured index  $n$  with the TO-phonon resonance centered at  $\omega_{\text{TO}}/2\pi = 8.13 \text{ THz}$  with a linewidth of  $\gamma/2\pi = 0.025 \text{ THz}$ , optical dielectric constant  $\epsilon_\infty = 5.13$ , and the TO-phonon strength  $\epsilon_{st} = 3.19$ . The good agreement between the measured data and fitting verifies the dominance of the TO-phonon resonance on the refractive index of ZnS. The power absorption was also fit to the TO-phonon line at 8.13 THz with various linewidth, however, it shows a weak effect compared to these observed TA-phonon resonance features.<sup>13</sup> The refractive index of ZnS at various temperatures in the range of  $17\text{--}74 \text{ cm}^{-1}$  (0.5–2.2 THz) has been studied previously by using channel spectrum technique.<sup>1</sup> We plot the previous data at room temperature by dots for comparison. It was fit with an undamped harmonic oscillator using parameters  $\omega_{\text{TO}}/2\pi = 7.80 \text{ THz}$ ,  $\epsilon_\infty = 4.7$ , and  $\epsilon_0 = \epsilon_\infty + \epsilon_{st} = 8.34$ .<sup>1</sup> Obviously, our results show a better correlation with the theoretical fit and demonstrate the efficiency of the THz-TDS characterizations and the accuracy with which it can determine the optical and dielectric parameters of the measured sample.

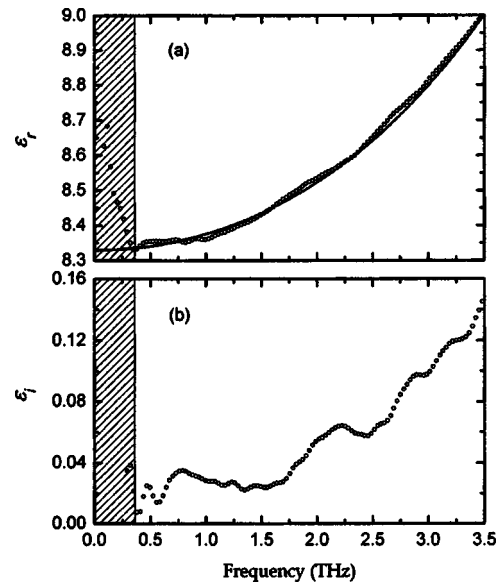


FIG. 2. Complex dielectric constant of single crystal ZnS: (a) measured real part of dielectric constant  $\epsilon_r$  (open circles) and the theoretical fitting (solid line); (b) measured imaginary dielectric constant  $\epsilon_i$ .

Based on the measured data of power absorption and refractive index we have extracted the frequency-dependent complex dielectric function of single crystal ZnS as shown in Fig. 2. The real and imaginary part of the dielectric constant are determined as  $\epsilon_r = n_r^2 - n_i^2 = n_r^2 - (\alpha\lambda_0/4\pi)^2$  and  $\epsilon_i = 2n_r n_i = \alpha n_r \lambda_0 / 2\pi$ . In Fig. 2(a), the real dielectric constant shows a feature that is essentially the square of the refractive index  $n_r$ . This is because the absorption by the sample is small in the spectral region concerned and the contribution of the absorption coefficient to the real dielectric constant is nearly negligible. The plot of the imaginary dielectric constant

Downloaded 28 Mar 2005 to 139.78.79.178. Redistribution subject to AIP license or copyright, see <http://apl.aip.org/apl/copyright.jsp>

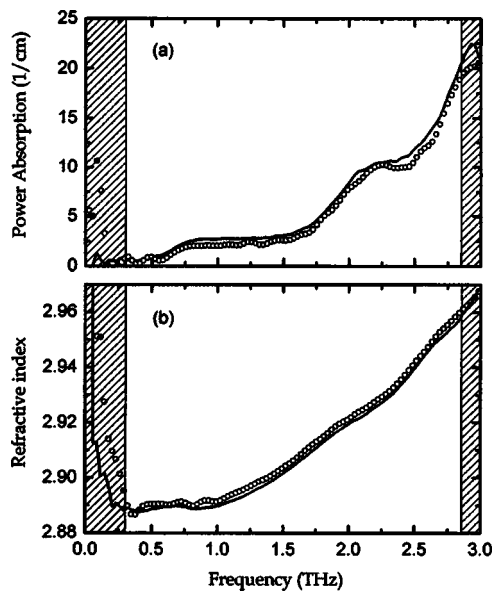


FIG. 3. (a) Measured power absorption coefficient of polycrystalline ZnS (solid line) compared with that of single crystal ZnS (open circles); (b) measured refractive index of polycrystalline ZnS (solid line) compared with that of single crystal ZnS (open circles).

shown in Fig. 2(b) has features similar to the power absorption curve but reveals the phonon resonance peaks more clearly. It therefore provides further verification of the phonon resonances determined by the power absorption and refractive index.

The procedure for the characterization of polycrystalline ZnS is essentially the same as that for single crystal ZnS sample. Figure 3(a) shows the absorption spectrum of polycrystalline ZnS. Due to the high absorption at higher frequencies and the relatively thick (3.42 mm) sample, the upper limit of the measured frequency range is reduced to 2.9 THz. Compared with the measured data for single crystal ZnS (open circles), the power absorption coefficient of polycrystalline ZnS is slightly higher, but clearly shows the similar phonon peaks at 0.78 and 2.20 THz, respectively. In contrast, the measured refractive index of polycrystalline ZnS (solid line) shown in Fig. 3(b) is slightly lower than that of single crystal ZnS (open circles). The frequency-dependent real and imaginary dielectric constant of polycrystalline ZnS are plotted in Fig. 4. Similar to the measured data for the single crystal sample, the phonon lines are clearly showing up in the imaginary dielectric constant of polycrystalline ZnS.

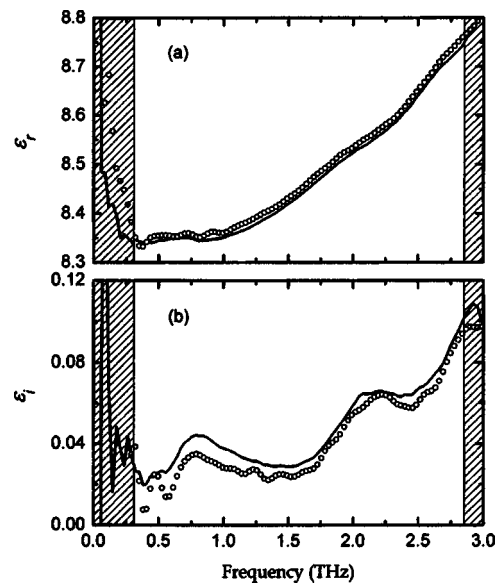


FIG. 4. (a) Real dielectric constant of polycrystalline ZnS (solid line) compared with that of single crystal ZnS (open circles); (b) imaginary dielectric constant of polycrystalline ZnS (solid line) compared with that of single crystal ZnS (open circles).

The authors acknowledge T. Collins and X. C. Xie for stimulating discussions and Kai Dou for kindly providing the polycrystalline ZnS sample. This work was partially supported by the Oklahoma EPSCoR for the National Science Foundation.

- <sup>1</sup>T. Hattori, Y. Homma, A. Mitsuishi, and M. Tacke, *Opt. Commun.* **7**, 229 (1973).
- <sup>2</sup>B. Y. Geng, L. D. Zhang, G. Z. Wang, T. Xie, Y. G. Zhang, and G. W. Meng, *Appl. Phys. Lett.* **84**, 2157 (2004).
- <sup>3</sup>S. Gupta, J. S. Meclure, and V. P. Singh, *Thin Solid Films* **33**, 299 (1997).
- <sup>4</sup>G. Gallot, J. Zhang, R. W. McGowan, T. I. Jeon, and D. Grischkowsky, *Appl. Phys. Lett.* **74**, 3450 (1999).
- <sup>5</sup>H. J. Bakker, G. C. Cho, H. Kurz, Q. Wu, and X.-C. Zhang, *J. Opt. Soc. Am. B* **15**, 1795 (1998).
- <sup>6</sup>Y. V. Korostelin, V. I. Kozlovsky, A. S. Nasibov, P. V. Shapkin, S. K. Lee, S. S. Park, J. Y. Han, and S. H. Lee, *J. Cryst. Growth* **184/185**, 1011 (1998).
- <sup>7</sup>W. Zhang, A. K. Azad, and D. Grischkowsky, *Appl. Phys. Lett.* **82**, 2841 (2003).
- <sup>8</sup>M. Born and E. Wolf, *Principles of Optics*, 7th (expanded) ed. (Cambridge University Press, Cambridge, UK, 2002), p. 65, Eq. (58).
- <sup>9</sup>W. G. Nilsen, *Phys. Rev.* **182**, 838 (1969).
- <sup>10</sup>G. A. Slack and S. Roberts, *Phys. Rev. B* **3**, 2613 (1971).
- <sup>11</sup>L. A. Feldkamp, G. Venkataraman, and J. S. King, *Solid State Commun.* **7**, 1571 (1969); J. Bergsma, *Phys. Lett.* **32A**, 374 (1970).
- <sup>12</sup>C. A. Klein and R. N. Donadio, *J. Appl. Phys.* **51**, 797 (1980).
- <sup>13</sup>N. Vagelatos, D. Wehe, and J. S. King, *J. Chem. Phys.* **60**, 3613 (1974).